Laser cooling, friction, and diffusion in a three-level cascade system

W. Rooijakkers,* W. Hogervorst, and W. Vassen
Department of Physics and Astronomy, Laser Centre Vrije Universiteit, De Boelelaan 1081, 1081 HV Amsterdam, the Netherlands
(Received 24 March 1997)

A model is presented to calculate optical forces, friction, and diffusion for three-level atoms in a ladder configuration. This model is then applied to the 2^3S_1-2^3P_2-3^3D_3 cascade in metastable helium. It is demonstrated that metastable helium atoms can be decelerated within a much shorter distance using cascade excitation by overlapping traveling waves. The equilibrium temperature representing the final width of the velocity distribution is calculated as a function of laser detuning and intensity. This equilibrium temperature is also calculated for the situation of overlapping standing waves (one-dimension), and is found to be well above the Doppler limit for two-level 2^3S_1-2^3P_2 excitation. Numerical results are compared with existing experimental data. [S1050-2947(97)03310-6]

PACS number(s): 32.80.Pj, 42.50.Vk

I. INTRODUCTION

First proposals for laser cooling of atoms started with the simplest situation of a two-level atom interacting with an external laser field. However, it was soon realized that the multi-level structure of atoms can be exploited to achieve much lower temperatures. One example of this is sub-Doppler polarization gradient cooling, which was theoretically described by Dalibard and Cohen-Tannoudji [1]. It is based on the delicate interplay of optical pumping between several Zeeman sublevels and the externally varying polarization. Another example is velocity selective coherent population trapping (VSCPT) [2]. In this scheme atoms are prepared in a coherent superposition of several Zeeman ground states such that they no longer interact with the light field. The latter is a necessary requirement for obtaining temperatures below the recoil limit.

Almost all of the theoretical and experimental work on multilevel laser cooling deals with systems displaying Zeeman degeneracy. In this paper we study laser cooling and diffusion in a three-level cascade. Examples of three-level cascade systems that may be considered are $3^2S_{1/2}\rightarrow 3^2P_{3/2}\rightarrow 3^2D_{5/2}$ in sodium (wavelengths 589 and 820 nm), $2^2S_{1/2}\rightarrow 2^2P_{3/2}\rightarrow 3^2D_{5/2}$ in lithium (wavelengths 671 and 610 nm), and $5^2S_{1/2}\rightarrow 5^2P_{3/2}\rightarrow 5^2D_{5/2}$ in rubidium (wavelengths 780 and 776 nm). In our calculations we will restrict ourselves to the $2^3S_1\rightarrow 2^3P_2\rightarrow 3^3D_3$ cascade in metastable helium (wavelengths 1083 and 588 nm).

Questions that may arise in such excitation processes are as follows: ''Can the cooling force be enhanced using an extra laser exciting the upper transition? Can the temperature in optical molasses be lowered by adding the second laser excitation? How large are friction and diffusion coefficients in cascade excitation?''

Zeeman degeneracy of the three-level cascade will not be considered. Such a degeneracy may give rise to complex cooling schemes similar in nature to polarization gradient cooling and VSCPT. We will focus on the phenomenology introduced by the use of an extra laser with a different frequency, exciting the atoms to a higher energy. For the two situations that we will discuss, excitation by overlapping traveling waves and excitation in one-dimensional two-color molasses (with overlapping standing waves), the atoms may always be prepared in an ideal three-level configuration, using optical pumping.

This paper is organized as follows. First we introduce the relevant parameters of this problem. We will describe the equations of motion for the internal states of the atom when recoil is neglected (optical Bloch equations). Characteristic parameters in laser cooling are friction and diffusion coefficients and we will give procedures to calculate these for the cascade system, including numerical examples for the case of metastable helium. Finally we will discuss experimental work by Kumakura and Morita who used cascade excitation of metastable helium atoms confined in a magneto-optical trap [3].

II. DESCRIPTION OF THE ATOM-FIELD SYSTEM

We consider a three-level system, with a ground state $|0\rangle$, an intermediate state $|1\rangle$, and an upper state $|2\rangle$ (see Fig. 1). The laser field $\mathbf{E}_1$ couples states $|0\rangle$ and $|1\rangle$; a second laser

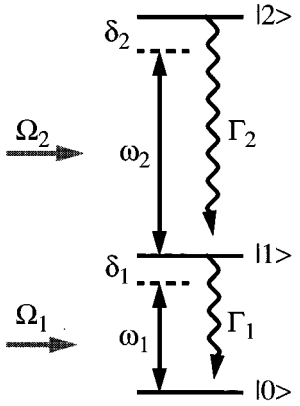

FIG. 1. Three-level atom interacting with two laser fields in a cascade configuration.

*Present address: Institut d'Optique Théorique et Appliquée, B.P. 147, 91403 Orsay, France.

field $\mathbf{E}_2$ states $|1\rangle$ and $|2\rangle$. There is no direct coupling between $|0\rangle$ and $|2\rangle$, i.e., the dipole moment $\langle 2|\mathbf{r}|0\rangle$ is zero. Thus the total electric field $\mathbf{E}$ may be written as

$$\mathbf{E}(\mathbf{R})=\mathbf{E}_1(\mathbf{R})\cos[\omega_1 t+\theta_1(\mathbf{R})]+\mathbf{E}_2(\mathbf{R})\cos[\omega_2 t+\theta_2(\mathbf{R})], \tag{1}$$

where $\mathbf{E}_i(\mathbf{R})$ is a spatially dependent amplitude of the electric field ($i=1,2$), and θ_i the phase of the respective field. The Hamiltonian for the system schematically shown in Fig. 1 is

$$H=H_A+H_V+V_{AL}+V_{AV}. \tag{2}$$

H_A represents the energy of the atomic system, containing both kinetic energy and internal energy, H_V represents the energy of the quantum (vacuum) radiation field. V_{AL} and V_{AV} are interaction terms of the atom with the laser field and the vacuum field, respectively. For the cascade system the interaction V_{AL} consists of two terms, one for each laser field present:

$$V_{AL}=-\mathbf{d}_1\cdot\mathbf{E}_1-\mathbf{d}_2\cdot\mathbf{E}_2. \tag{3}$$

Here $\mathbf{d}_1$ and $\mathbf{d}_2$ are the dipole moments for the two transitions in the cascade. It is common to introduce Rabi frequencies to describe the strength of the laser field:

$$\Omega_i(\mathbf{R})=\mathbf{d}_i\cdot\mathbf{E}_i(\mathbf{R})/\hbar. \tag{4}$$

The interaction of the excited atom with the vacuum fields leads to spontaneous emission which we will treat phenomenologically throughout this paper. The transition rates for radiative decay of the intermediate and upper level are given by

$$\Gamma_i=d_i^2\omega_i'^3/(3\pi\varepsilon_0\hbar c^3). \tag{5}$$

Here ω_i' is the atomic transition frequency. The difference between the laser frequency ω_i and the atomic transition frequencies ω_i' is the detuning δ_i:

$$\delta_i=\omega_i-\omega_i'. \tag{6}$$

Equations (4), (5), and (6) define the fundamental parameters in our context of cascade laser cooling and its semiclassical description. We will derive friction and diffusion coefficients which in principle depend on these six parameters. This large number of parameters makes it hard to search for optimized forces or temperatures. For a specific atom the transition linewidths are known, resulting in a remaining set of four adjustable parameters.

III. EQUATIONS OF MOTION FOR THE INTERNAL STATE OF THE ATOM

The time evolution of the internal state of the atom (neglecting recoil) is described by optical Bloch equations (OBE's), which in their most general form are written as

$$\frac{d}{dt}\hat{\rho}=\frac{1}{i\hbar}[\hat{H},\hat{\rho}]+\hat{\rho}_{\text{relax}}, \tag{7}$$

where $\hat{\rho}$ is the density matrix operator of the system. Throughout this paper a circumflex is written to emphasize that the corresponding symbol represents a quantum-mechanical operator, containing ket-bra projection operators, e.g., $\hat{\rho}_{ij}=|j\rangle\langle i|$. When the operator form is not shown explicitly, the symbol represents an expectation value, e.g., $\rho_{ij}=\mathrm{Tr}[\hat{\rho}\cdot\hat{\rho}_{ij}]=\langle\hat{\rho}_{ij}\rangle$. Using the rotating wave approximation, the full set of nine equations that appear in the three-level cascade case, including the relaxation terms due to spontaneous emission, have been worked out by Whitley and Stroud [4]. This set of equations takes the following form:

$$\frac{d\mathbf{x}}{dt}=A\cdot\mathbf{x}. \tag{8}$$

Here A is a 9×9 matrix containing the six parameters in the problem (linewidths, Rabi frequencies, and detunings) and $\mathbf{x}$ is a column vector containing the nine expectation values for the density matrix elements [Whitley and Stroud take $\mathbf{x}=(\rho_{22},\rho_{21},\rho_{20},\rho_{10},\rho_{00},\rho_{01},\rho_{02},\rho_{12},\rho_{11})$]. In a steady-state situation the left-hand side of Eq. (8) is zero, resulting in a set of linear equations. Since this system is overdetermined, one of the equations may be cancelled and be replaced by the condition that the sum of all populations equals one ($\rho_{00}+\rho_{11}+\rho_{22}=1$). This results in a set of nine independent equations that formally may be described as

$$\left[\frac{d\mathbf{x}}{dt}\right]_p=A_p\cdot\mathbf{x}. \tag{9}$$

The subindex p refers to the fact that one of the rows in the matrix A has been changed. Thus analytical expressions may be found for the steady-state values of the density matrix elements ρ_{ij} ($0\leqslant i,\ j\leqslant 2$). These expressions are given explicitly in an appendix of the Whitley and Stroud paper [4]. They are rather lengthy and are not reproduced here.

We prefer to cast the optical Bloch equations of Whitley and Stroud into a different form, using the following transformation:

$$\begin{aligned}
&u_{01}=\rho_{01}+\rho_{10}, && u_{12}=\rho_{12}+\rho_{21}, && u_{13}=\rho_{02}+\rho_{20},\\
&v_{01}=-i(\rho_{01}-\rho_{10}), && v_{12}=-i(\rho_{12}-\rho_{21}), && v_{13}=-i(\rho_{02}-\rho_{20}),\\
&w_{01}=\rho_{00}-\rho_{11}, && w_{12}=\rho_{11}-\rho_{22}. &&
\end{aligned} \tag{10}$$

This approach has several advantages. The parameters (u,v,w) correspond to the real part of the atomic polarization, the imaginary part of the atomic polarization and the atomic inversion, respectively. As we shall explain the expressions for optical forces on the atom take their simplest form using the (u,v,w) parametrization; the two types of forces identified, i.e., the

dissipative spontaneous emission force and the reactive dipole force correspond to the imaginary and real part of the atomic polarization, respectively [5]. The optical Bloch equations now contain only real terms and take the form

$$\frac{d\mathbf{y}}{dt} = B \cdot \mathbf{y} + \mathbf{b}, \tag{11}$$

where the matrix B is given by

$$B = \begin{bmatrix} -\Gamma_1 & \delta_1 & 0 & 0 & 0 & 0 & 0 & \frac{\Omega_2}{2} \\ -\delta_1 & -\Gamma_1 & -\Omega_1 & 0 & 0 & 0 & -\frac{\Omega_2}{2} & 0 \\ 0 & \Omega_1 & \frac{2\Gamma_2 - 4\Gamma_1}{3} & 0 & -\frac{\Omega_2}{2} & \frac{4\Gamma_1 + 4\Gamma_2}{3} & 0 & 0 \\ 0 & 0 & 0 & -\Gamma_1 - \Gamma_2 & \delta_2 & 0 & 0 & -\frac{\Omega_1}{2} \\ 0 & 0 & 0 & -\delta_2 & -\Gamma_1 - \Gamma_2 & -\Omega_2 & \frac{\Omega_1}{2} & 0 \\ 0 & -\frac{\Omega_1}{2} & \frac{2\Gamma_1 - 4\Gamma_2}{3} & 0 & \Omega_2 & -\frac{2\Gamma_1 + 8\Gamma_2}{3} & 0 & 0 \\ 0 & \frac{\Omega_2}{2} & 0 & 0 & -\frac{\Omega_1}{2} & 0 & -\Gamma_2 & \delta_1 + \delta_2 \\ -\frac{\Omega_2}{2} & 0 & 0 & \frac{\Omega_1}{2} & 0 & 0 & -\delta_1 - \delta_2 & -\Gamma_2 \end{bmatrix} \tag{12}$$

and the inhomogeneous vector **b** by

$$\mathbf{b} = \left(0,0, \frac{4\Gamma_1 - 2\Gamma_2}{3}, 0,0, \frac{4\Gamma_2 - 2\Gamma_1}{3}, 0,0 \right). \tag{13}$$

The vector $\mathbf{y} = (u_{01}, v_{01}, w_{01}, u_{12}, v_{12}, w_{12}, u_{02}, v_{02})$ contains the density matrix information. The steady-state solution of Eq. (11) (for a nonmoving atom at position **R**) can be found analytically, but in general the expressions for the elements of **y** are rather lengthy [6]. In the limit where the upper transition is not excited ($\Omega_2 = 0$) the above set reduces to four equations. After elimination of the w_{12} term, the familiar set of three OBE's for the two level system is obtained.

For zero detuning and high intensities ($\delta_1 = \delta_2 = 0$; $\Omega_{1,2} \gg \Gamma_{1,2}$) Cohen-Tannoudji and Reynaud found a dressed-atom basis [7]. This allows for a better physical understanding in this limiting situation and a direct calculation of the populations. The advantage of a dressed-atom approach vanishes for nonzero detuning as the complexity of the expressions then becomes comparable to those of the OBE approach.

Now that we have a full description of the atomic density matrix we may calculate expectation values for any quantum-mechanical operator $\hat{O}$, using the well known identity $\langle \hat{O} \rangle = \mathrm{Tr}[\hat{\rho}\, \hat{O}]$. We will proceed in the next paragraphs by writing down expressions for the force operator. Values for diffusion and friction cannot directly be calculated by tracing over the density matrix, since they contain *two-time* correlations between the density matrix elements. This necessitates that we take into account the unitary evolution of the complete system (including the vacuum reservoir). This will be explained in more detail in Sec. VI.

IV. OPTICAL FORCES IN THE CASCADE SYSTEM

The center-of-mass motion of the atom can be described by the Heisenberg equations for the position **R** and the momentum **P** [5,8–10]. The velocity of the center of mass is given by

$$\dot{\mathbf{R}} = \frac{1}{i\hbar}[\mathbf{R}, H] = \frac{\partial H}{\partial \mathbf{P}} = \frac{\mathbf{P}}{M}. \tag{14}$$

The force operator $\mathbf{F}(\mathbf{R}) = M\ddot{\mathbf{R}} = \dot{\mathbf{P}}$ is given by the Heisenberg equation for **P**:

$$\dot{\mathbf{P}} = \frac{1}{i\hbar}[\mathbf{P}, H] = -\frac{\partial H}{\partial \mathbf{R}}. \tag{15}$$

Using Eq. (2) we find

$$\hat{\mathbf{F}}(\mathbf{R}) = -\nabla \hat{V}_{AL}(\mathbf{R}) - \nabla \hat{V}_{AV}(\mathbf{R}). \tag{16}$$

It may be shown that the second term vanishes in the quasiclassical calculation of the mean force. However, this term gives a significant contribution to the diffusion, as will be described later. Using $\mathbf{d}_1 = d_1 \mathbf{e}_z (|0\rangle\langle 1| + |1\rangle\langle 0|)$ and a similar expression for $\mathbf{d}_2$, and using Eqs. (3) and (4), dropping the counter-rotating terms, we find the following expression:

$$\hat{V}_{AL}=\frac{\hbar\Omega_1(\mathbf{R})}{2}\,[e^{-i\theta_1(\mathbf{R})}e^{-i\omega_1 t}|1\rangle\langle 0|+\text{H.c.}]$$

$$+\frac{\hbar\Omega_2(\mathbf{R})}{2}\,[e^{-i\theta_2(\mathbf{R})}e^{-i\omega_2 t}|2\rangle\langle 1|+\text{H.c.}]. \quad (17)$$

Here it has been assumed that the laser fields may be written as $\mathbf{E}_i(\mathbf{r},t)=\boldsymbol{\epsilon}_i(\mathbf{r})\mathcal{E}_i(\mathbf{r})\cos[\omega_i t-\theta_i(\mathbf{r})]$, where $\boldsymbol{\epsilon}_i(\mathbf{r})$ and $\mathcal{E}_i(\mathbf{r})$ are the spatially dependent polarization and amplitude of the field, respectively [5]. Inserting Eq. (17) into Eq. (16), and using the operator form of Eq. (11), we get the following expression for the cascade force expectation value:

$$F_{\text{cascade}}=\frac{\hbar}{2}\,(u_{01}\nabla\Omega_1+v_{01}\Omega_1\nabla\theta_1)$$

$$+\frac{\hbar}{2}\,(u_{12}\nabla\Omega_2+v_{12}\Omega_2\nabla\theta_2). \quad (18)$$

The average force thus consists of four terms, the first two corresponding to the lower transition, the last two to the upper. As in a two-level system the force can be split into a phase gradient part corresponding to radiation pressure and an intensity gradient part corresponding to a dipole force. It is easily seen that this picture can be generalized to multilevel cascade systems. We shall see later that contributions to the diffusion do not necessarily add up for the different transitions, i.e., cross terms may appear.

For overlapping plane traveling waves the intensity gradient part vanishes and the phases are given by $\theta_i=\mathbf{k}_i\cdot\mathbf{R}$ with $k_i=2\pi/\lambda_i$ the wave vector of the laser radiation. Using Eqs. (10), (11), and (18), we find the following expression for the average radiation force:

$$F_{\text{rad}}=\hbar k_1\Gamma_1\rho_{11}+\hbar k_2\Gamma_2\rho_{22}. \quad (19)$$

The radiation force in Eq. (19) can be easily understood: the terms on the right-hand side correspond to the momentum change that is caused by the fact that a photon $\hbar k$ is always absorbed in one direction whereas it is spontaneously emitted in a random direction. The rate of photons scattered is given by the upper state population for each transition divided by its average lifetime. Equation (19) has been experimentally tested for metastable helium [11]. For this atom the second term can be made much larger than the first one, which allows for a theoretical enhancement of the radiation force by almost an order of magnitude compared to a two-level system. To test this an atomic beam of metastable helium atoms was perpendicularly crossed by two overlapping traveling waves exciting the cascade. The deflection of the atomic beam as a result of the radiation force was measured, and it was found that the deflection for two-color excitation could be made a factor of 8 larger than the maximum deflection for one-color (two-level) excitation. Moreover, the behavior of the force enhancement as a function of laser intensities was shown to be in agreement with the model outlined above.

We point out that the term bichromatic cooling has also been used in the literature for describing a situation of overlapping *standing* waves, where the phase gradient is absent. Grove *et al.* [12] have described such a situation in a cascade level system in rubidium, deriving a position dependent force which may also exceed the maximum spontaneous emission force for the two-level system.

V. FRICTION AND DIFFUSION

So far we have described the internal motion of the atom ignoring recoil. For a study of laser-cooling processes, however, the external degrees of freedom are relevant as well, and must be included in the density matrix formalism. Formal procedures exist to derive evolution equations for the phase-space distribution of a statistical sample of atoms. A comparison of semiclassical and fully quantum-mechanical approaches to this problem is given by Dalibard and Cohen-Tannoudji [13]. We will use the semiclassical expressions used by Cook [8] and Gordon and Ashkin [10] for a two-level system. These expressions were also applied by Ungar *et al.* [14], Nienhuis, van der Straten, and Shang [15], and Mølmer [16] to systems displaying Zeeman structure. It can be shown that under certain conditions (de Broglie wavelength of the atom much smaller than the laser wavelength and $\hbar\Gamma\gg\hbar^2k^2/2M$ [5]) the evolution of the distribution function in phase space $f(\mathbf{R},\mathbf{P})$ may be described by a Fokker-Planck equation [17]:

$$\frac{\partial f}{\partial t}=-\frac{\mathbf{P}}{M}\frac{\partial f}{\partial\mathbf{R}}-\frac{\partial}{\partial\mathbf{P}}\,(\mathbf{F}f)+\frac{\partial^2}{\partial P^2}\,(\overline{D}f). \quad (20)$$

The right-hand side of this equation shows three terms. The first is a hydrodynamic term which describes the free spatial evolution of the distribution, given its velocity. This term may be included on the left-hand side of the equation using a total derivative instead of a partial derivative. The second term represents the effect of the mean (cooling) force $\mathbf{F}$ on the phase-space distribution. If the phase space distribution is sufficiently confined in momentum, this mean force may be linearized: $\mathbf{F}=-\overline{\alpha}(\mathbf{P}/M)=-\overline{\alpha}\mathbf{v}$ where $\overline{\alpha}$ is called the friction tensor ($\overline{\alpha}$ is used instead of α to emphasize the tensorial character). The third term in Eq. (20) describes the effect of fluctuations in the optical force. These fluctuations are represented by the diffusion tensor $\overline{D}$, given by

$$2\overline{D}=\frac{\langle(\Delta\hat{P}-\langle\Delta\hat{P}\rangle)^2\rangle}{\Delta t}$$

$$=\int_{-\infty}^{\infty}[\langle\hat{\mathbf{F}}(\tau)\hat{\mathbf{F}}(0)\rangle-\langle\hat{\mathbf{F}}(0)\rangle\langle\hat{\mathbf{F}}(\tau)\rangle]\,d\tau. \quad (21)$$

Diffusion may thus be expressed in terms of two-time force correlations, and special techniques have to be employed to calculate expressions of the type $\langle\hat{A}(t_1)\hat{B}(t_2)\rangle$ [18]. Symmetry allows us to integrate the above expression starting from time zero. We assume that the atom is in the steady state at time $\tau=0$ so that we may replace $\langle\hat{\mathbf{F}}(\tau)\rangle\langle\hat{\mathbf{F}}(0)\rangle$ with $\langle\hat{\mathbf{F}}(0)\rangle\langle\hat{\mathbf{F}}(0)\rangle$ [19], resulting in

$$\overline{D}=\text{Re}\int_0^{\infty}[\langle\hat{\mathbf{F}}(\tau)\hat{\mathbf{F}}(0)\rangle-\langle\hat{\mathbf{F}}(0)\rangle\langle\hat{\mathbf{F}}(0)\rangle]\,d\tau. \quad (22)$$

In the rest of this paper we limit ourselves to a one-dimensional situation, implying that we only consider a diffusion scalar D rather than a tensor $\overline{D}$.

The total diffusion coefficient may be written as the sum of two contributions: $D_{\mathrm{tot}}=D_{\mathrm{corr}}+D_{\mathrm{spon}}$. The second term is due to spontaneous emission which must be dealt with separately if the atom-vacuum interaction [V_{AV} in Eq. (2)] is not included in the derivation of the force operator [Eq. (16)]. The result for the cascade system, extending the two-level result, becomes [8]

$$D_{\mathrm{spon}}=\frac{1}{10}(\hbar k_1)^2\Gamma_1\rho_{11}+\frac{1}{10}(\hbar k_2)^2\Gamma_2\rho_{22}. \tag{23}$$

The factor 1/10 is due to the fact that spontaneous emission is nonisotropic in three dimensions [8,15] (the factor for the diffusion coefficient in a direction perpendicular to the induced dipole moment is a factor of 2 larger, i.e., 1/5 instead of 1/10). For the specific case of metastable helium the second term at the right-hand side of Eq. (23) becomes dominant in case of sufficient population of the upper level ($\rho_{22}>0.05$). D_{spon} cannot exceed a certain value determined by the atomic parameters, contrary to the term D_{corr} which generally dominates for situations with high laser intensity (in which case the total diffusion becomes proportional to the Rabi frequency, as it determines the rate at which photons are transferred to different modes by stimulated emission).

D_{corr} accounts for the stochastics in the laser-atom interaction. We will calculate this term following the prescription of Mølmer and Agarwal [16,20]. The force operator may be formally expressed as

$$\hat{F}(\mathbf{R},\tau)=\sum_{ij}F_{ij}(\mathbf{R})|j\rangle\langle i|(\tau)=\sum_{ij}F_{ij}(\mathbf{R})\hat{\rho}_{ij}(\tau). \tag{24}$$

In accordance with the Heisenberg picture the projection operators $|j\rangle\langle i|$ depend on time τ (in contrast with the Schrödinger picture, where the system eigenstates are time-dependent instead of the operators). Equation (22) may be rewritten as

$$\begin{aligned}D(\mathbf{R})&=\mathrm{Re}\sum_{ijkl}F_{ij}(\mathbf{R})F_{kl}(\mathbf{R})\int_0^\infty[\langle\hat{\rho}_{ij}(\tau)\hat{\rho}_{kl}(0)\rangle\\&\quad-\langle\hat{\rho}_{ij}(0)\rangle\langle\hat{\rho}_{kl}(0)\rangle]d\tau\\&=\mathrm{Re}\sum_{ijkl}F_{ij}(\mathbf{R})F_{kl}(\mathbf{R})\int_0^\infty\phi_{ijkl}(\mathbf{R},\tau)d\tau,\end{aligned} \tag{25}$$

with the indices i,j,k,l running over all levels of the cascade. According to the quantum regression theorem (see, e.g., [21]), the quantities ϕ_{ijkl} follow the same equations of motion as the expectation values for the elements of the density matrix [Bloch equations (8)]:

$$\dot{\phi}_{kl}(\mathbf{R},\tau)=A(\mathbf{R})\phi_{kl}(\mathbf{R},\tau). \tag{26}$$

Here $A(\mathbf{R})$ is the same matrix as in Eq. (8), and the ϕ_{ijkl} are grouped in a vector $\boldsymbol{\phi}_{kl}$. The elements in this vector are positioned using the label i,j the same way as convened in Eq. (8): $\boldsymbol{\phi}_{kl}=(\phi_{22kl},\phi_{21kl},\phi_{20kl},\phi_{10kl},\phi_{00kl},\phi_{01kl},\phi_{02kl},\phi_{12kl},\phi_{11kl})$.Each possible combination of labels k,l requires a new evaluation of Eq. (26). Now the integral in Eq. (25) can be calculated, using $\phi_{ijkl}(\mathbf{R},\infty)=0$:

$$\int_0^\infty\phi_{kl}(\mathbf{R},\tau)d\tau=-A_p^{-1}(\mathbf{R})\phi_{kl}(\mathbf{R},0)_p. \tag{27}$$

The Bloch matrix $A_p(\mathbf{R})$ is the same as in Eq. (9). The subindex p refers to the insertion of the condition that the integral of ϕ_{ijkl} has zero trace [16], the corresponding element in $\boldsymbol{\phi}_{kl}(\mathbf{R},0)_p$ should thus be a zero. The vector $\boldsymbol{\phi}_{kl}(\mathbf{R},0)$ containing the initial values ($\tau=0$) can be calculated using one-time expectation values for the density matrix, given by Eq. (9):

$$\phi_{ijkl}(\mathbf{R},0)=\rho_{jk}(\mathbf{R})\delta_{il}-\rho_{ij}(\mathbf{R})\rho_{kl}(\mathbf{R}). \tag{28}$$

The delta function arises from the fact that the projection operator $|l\rangle\langle k|(0)$ is followed by the projection operator $|j\rangle\langle i|(0)$ before calculating the expectation value, and $\langle i|l\rangle=\delta_{il}$ (orthogonal and normalized states). As a consequence the diffusion coefficient in a system containing more than two levels *cannot* be considered as consisting of independent terms for the respective transitions, or in other words cross terms will appear and may be significant.

To clarify the implication of this we use the paradigm of the drunkard, who takes steps with a fixed size in random directions and at random times, thereby moving away from his original position. Consider now a more complex situation where the drunkard can make either big or small steps. If the stepsize is independent of history, i.e., the steps are not correlated, we may estimate the most probable distance the drunkard covered since he left his original position using the theory for the case of only one possible stepsize. However, if a big step is likely to be followed by a small one or vice versa, the characteristics of that correlation have to be taken into account. In our description of cascade excitation it is the coherence of both lasers that provides a correlation between the random steps with sizes $\hbar k_1$ and $\hbar k_2$ in momentum space. It is thus not surprising that the optical Bloch equations contain all the information on the time correlation between the steps, as exploited using the quantum regression theorem. This correlation only exists for absorption and stimulated emission processes. The random steps due to spontaneous emission are not correlated, i.e., the correlation time between the atom and the vacuum radiation field reservoir is much shorter than the typical time scale for the evolution of the atom. For this reason Eq. (23) only involves the two-level (single-step size) result.

Similarly to Eq. (25) for the diffusion, an expression for the friction coefficient is found [13]:

$$\alpha(\mathbf{R})=\frac{-2}{\hbar}\,\mathrm{Im}\sum_{ijkl}F_{ij}(\mathbf{R})F_{kl}(\mathbf{R})\int_0^\infty\tau\phi_{ijkl}(\mathbf{R},\tau)d\tau. \tag{29}$$

The integral in Eq. (29) can be found [16] by using Eq. (27) in combination with the following equation:

$$\int_0^\infty\tau\phi_{kl}(\mathbf{R},\tau)d\tau=-A_p^{-1}(\mathbf{R})\left[\int_0^\infty\phi_{kl}(\mathbf{R},\tau)d\tau\right]_p. \tag{30}$$

Friction and diffusion coefficients are important parameters to characterize a statistical sample of atoms in the semiclassical approximation. The spatially averaged friction and dif-

fusion coefficients may be used to calculate an equilibrium temperature T (assuming that these coefficients are not a function of velocity over the full width of the velocity distribution of the considered sample of atoms):

$$k_B T = \frac{D_{\text{tot}}}{\alpha}. \tag{31}$$

This equation is only meaningful for positive α (with the force defined as $F = -\alpha v$). Diffusion and friction can be calculated from Eq. (25) and Eq. (29), respectively, inserting Eq. (27), (28), and (30). The calculation procedure is straightforward and only involves the repeated use of the inverted Bloch matrix A_p^{-1}, which is reasonably small (9×9 elements) for the three-level cascade system. However, in the case of standing waves the matrix is a function of position, and the expressions should be evaluated over a full unit cell of the standing wave pattern of the laser fields, to obtain average values. For overlapping standing waves in the cascade system averaging is more delicate than for a single standing wave. A much larger distance containing both an integer number of wavelengths for the upper and for the lower transition must be used in the averaging process. We have used a grid $N = 100$ covering this distance. In the next paragraph we will present our numerical results for the case of overlapping standing waves in one dimension, exciting the three-level cascade.

VI. NUMERICAL CALCULATION OF FRICTION AND DIFFUSION COEFFICIENTS IN ONE DIMENSION

Using the theory described in the previous paragraph we have calculated friction and diffusion coefficients for one-dimensional overlapping traveling waves and standing waves. Except for detuning which is given in MHz, our results are represented in dimensionless scaled quantities: Rabi frequencies are divided by the linewidth of the corresponding transition, forces by $\hbar k_1 \Gamma_1/2$ (which is the maximum radiation force for a two-level system), diffusion and friction coefficients by $(\hbar k_1)^2 \Gamma_1/4$ and $\hbar k_1^2 \Gamma_1/4$, respectively, which are the maxima in a two-level traveling wave situation. Temperature is scaled to the two-level Doppler limit $\hbar \Gamma_1/2$. The linewidths were chosen for the metastable helium atom ($1/\Gamma_1 = 98$ nsec; $1/\Gamma_2 = 14$ nsec).

When Ω_2 is small the two-level limit of three-level cascade excitation is reached. We verified that our computing code reproduces the two-level results of Gordon and Ashkin [10] and Cook [8]. It was also verified that the number of positions used to average over a standing wave pattern was sufficient, i.e., a further increase of this number ($N = 100$) gave no different results (convergence criterion).

A. Numerical results for two-color deceleration using traveling waves

As explained in Sec. IV, the radiation force on metastable helium can be increased by an order of magnitude using cascade excitation. It is interesting to consider deceleration of these atoms within a reduced distance using this enhanced force. An atom moving with velocity $\mathbf{v}$ in the laboratory frame experiences a Doppler shift $\mathbf{k} \cdot \mathbf{v}$. For cascade excitation by two overlapping laser beams, counterpropagating with the atomic beam, it is necessary to consider two Doppler shifts $\mathbf{k}_1 \cdot \mathbf{v}$ and $\mathbf{k}_2 \cdot \mathbf{v}$. As the atoms decelerate, the Doppler shifts change, and the laser frequencies should be adjusted synchronously to maintain a large force. This technique is known as frequency chirping [22]. Consider a situation where the optical force is kept maximum for a velocity v_0 which varies linearly with time t. This is realized by imposing $\delta_1(t) = \mathbf{k}_1 \cdot \mathbf{v}_0(t)$ and $\delta_2(t) = \mathbf{k}_2 \cdot \mathbf{v}_0(t)$ corresponding to a frame with deceleration $a_{\text{chirp}} = dv_0/dt$ with respect to the laboratory inertial frame. In order to deal with the force fluctuations (represented by a diffusion coefficient) a_{chirp} should be chosen smaller than $a_{\max} = F_{\max}/M$, where $F_{\max}$ is the maximum value of the velocity dependent optical force $F(v - v_0)$. In that case it may be shown [23] that atoms will accumulate around a momentary velocity $v_s(t)$, given by $F(v_s - v_0) = M a_{\text{chirp}}$ ($v_s > v_0$). The velocity distribution around v_s evaluates to a width Δv, given by $M(\Delta v)^2 = D/\alpha = k_B T$ [see Eqs. (20) and (31)]. Here it is assumed that D and α are almost constant over the interval Δv around v_s. Taking $a_{\text{chirp}} < a_{\max}$ ensures locking of the atoms to the decelerating frame: an atom which—due to a fluctuation in the force—has shifted from v_s towards v_0 will feel an inertial force pushing it back to its equilibrium velocity v_s. This is of course only true when the excursion of the atom has not exceeded the velocity range for which $F(v - v_0) > M a_{\text{chirp}}$. Usually the choice of a_{chirp} is based on a compromise by increasing this velocity ''capture'' range and avoiding a too large reduction in stopping distance. A typical choice is $a_{\text{chirp}} = a_{\max}/2$.

Force, friction, and diffusion have been calculated as a function of velocity for the case of metastable helium deceleration. It was assumed that the atoms are resonant with the laser frequencies at $v = v_0$. This was performed for several intensities of the decelerating laser beams. For each given Rabi frequency Ω_1 of the lower transition, we calculated the corresponding Rabi frequency Ω_2 for the upper transition that would give the maximum population in the upper level. The results are shown in Fig. 2. The velocity capture range Δv_c of the force can be defined as the full width at half maximum of the bell shaped curve (the force curves are symmetric around $v = v_0$). As expected the capture range increases with increasing laser power (comparable to power broadening for a two-level system).

It should be noted that—contrary to the case of standing waves—there is no spatial dependence of the force to be averaged over. Thus the friction coefficient is simply the derivative of the force: $\alpha = dF/dv$. Rather than taking this derivative, we have used Eq. (29) since it does not require evaluation at two different points in (velocity) space.

We may formally calculate an equilibrium temperature for a velocity distribution peaked around $v = v_s$. This is also shown in Fig. 2. The temperature increases with laser intensity. Using the fact that the temperature is scaled to the two-level Doppler limit, we may calculate $\langle \Delta v \rangle$ by taking the square root of the value along the vertical axis in the temperature curve of Fig. 2, multiplied by the velocity corresponding to the one-dimensional Doppler limit for metastable helium ($v_{\text{Doppler}} = 0.39$ m/s). Doing this it is found that for all the situations considered $\langle \Delta v \rangle$ is smaller than Δv_c by at least one order of magnitude, assuring the accumulation of atoms in the decelerating frame. This demonstrates the fea-

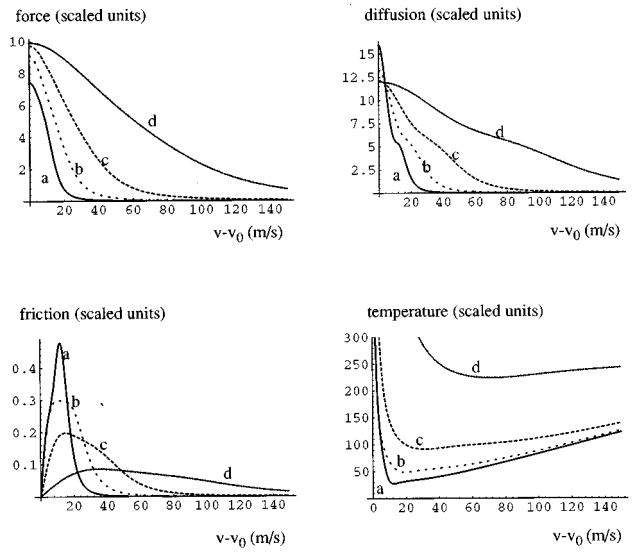

FIG. 2. Force, friction, diffusion, and equilibrium temperature as a function of velocity for overlapping traveling waves exciting the three-level cascade in metastable helium. Curves correspond to (*a*) $\Omega_1=3\Gamma_1$, $\Omega_2=1.4\Gamma_2$; (*b*) $\Omega_1=6\Gamma_1$, $\Omega_2=2.2\Gamma_2$; (*c*) $\Omega_1=12\Gamma_1$, $\Omega_2=3.7\Gamma_2$; (*d*) $\Omega_1=31\Gamma_1$, $\Omega_2=8.9\Gamma_2$.

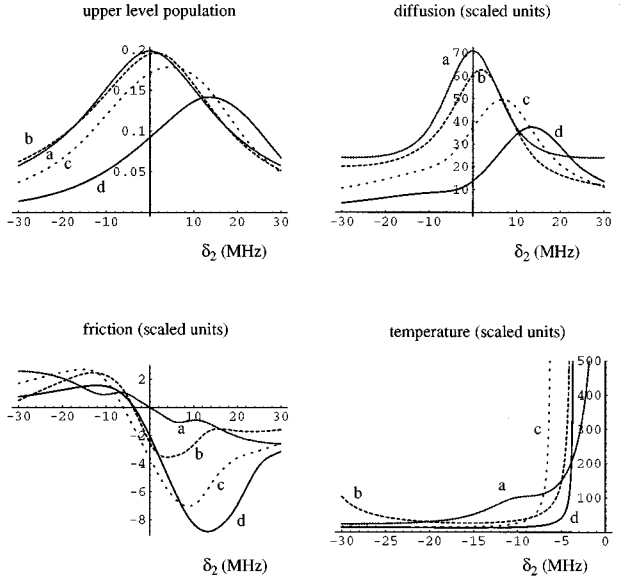

FIG. 3. Numerical calculation of average upper level population, diffusion coefficient, friction coefficient, and equilibrium temperature for three-level cascade excitation of metastable helium atoms in one-dimensional overlapping standing waves, in the case of strong upper transition excitation ($\Omega_2=1.9\Gamma_2$). Curves are (*a*) $\delta_1=0$; (*b*) $\delta_1=-5$ MHz; (*c*) $\delta_1=-15$ MHz; (*d*) $\delta_1=-25$ MHz. Averaged over position (see text).

sibility of two-color deceleration using simultaneous frequency chirping.

B. Numerical results for two-color overlapping standing waves

It is also of interest to study the behavior of friction and diffusion in one-dimensional molasses varying the detunings of the two lasers. Another important parameter is the intensity (Rabi frequency) of the laser field exciting the upper transition. We have investigated two regimes, one of reasonably strong upper level excitation ($\Omega_2=1.9\Gamma_2$), and another with weak excitation ($\Omega_2=0.4\Gamma_2$), in which case the results should represent a perturbation of the two-level system (in both cases $\Omega_1=5.5\Gamma_1$, corresponding to strong saturation of the lower transition).

For weak excitation (Fig. 4) the population of the upper level is favorable at two-photon resonance, where the positive detuning of the lower transition laser frequency is compensated by the negative detuning of the upper exciting laser field. This two-photon resonance condition does not hold in the case of strong excitation (Fig. 3) as the Rabi frequencies are not negligible against the detunings. In general there is a competition between the Rabi frequencies and detunings used in the matrix Eq. (12). A high Rabi frequency for the upper transition may Stark shift the intermediate level which results in an effective detuning δ_{eff} different from δ_1.

Our diffusion results are shown in Fig. 3 (strong excitation) and Fig. 4 (weak excitation), with the detuning of the upper transition laser field (δ_2) plotted along the horizontal axis. As expected an increased excitation of the upper level leads to an increased diffusion in the case of strong upper transition excitation (Fig. 3). The diffusion does not approach zero for $|\delta_2|\to\infty$, due to the remaining diffusion caused by relatively strong excitation of the lower transition. As can be seen a detuning δ_1 of the lower laser transition takes away the symmetry around $\delta_2=0$. In contrast with the diffusion curves for strong upper level excitation, the diffusion for weak upper level excitation (Fig. 4) *decreases* for $\delta_1=0$, $|\delta_2|\to 0$. This effect may be explained by coherent population trapping [19,24,25], in which case part of the atoms reside in a state $|\text{NC}\rangle$ that is not coupled to the laser light $\hat{V}_{AL}|\text{NC}\rangle=0$:

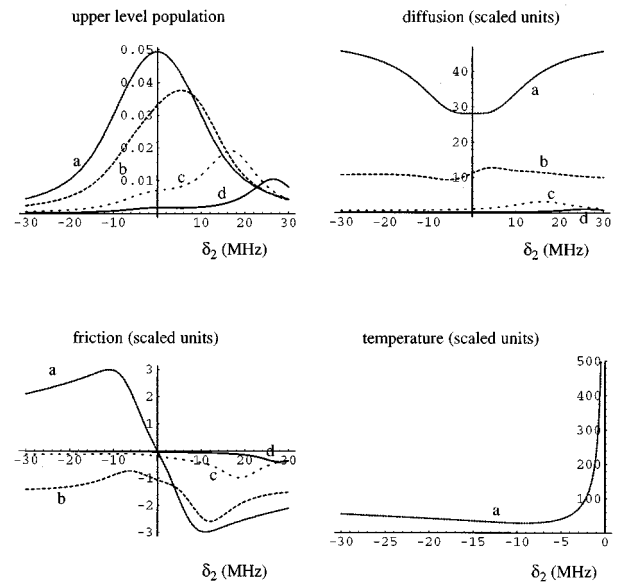

FIG. 4. Numerical calculation of average upper level population, diffusion coefficient, friction coefficient, and equilibrium temperature for three-level cascade excitation of metastable helium atoms in one-dimensional overlapping standing waves, in the case of weak upper transition excitation ($\Omega_2=0.4\Gamma_2$). Curves are (*a*) $\delta_1=0$; (*b*) $\delta_1=-5$ MHz; (*c*) $\delta_1=-15$ MHz; (*d*) $\delta_1=-25$ MHz. Averaged over position (see text).

$$|\mathrm{NC}\rangle = \frac{1}{\sqrt{\Omega_1^2+\Omega_2^2}}\,(\Omega_2|0\rangle - \Omega_1|2\rangle). \tag{32}$$

Contrary to the dark state in a lambda system [2], the dark state in Eq. (32) is not stable against spontaneous emission. In a steady-state situation, however, a substantial fraction of the atoms, given by $(\Omega_1\rho_{22}-\Omega_2\rho_{00})^2/(\Omega_1^2+\Omega_2^2)$, will be pumped into this superposition state ($\delta_1=\delta_2=0$). Since there is no force on atoms in a noncoupled state, the diffusion D_{corr} has vanished for this fraction.

Friction coefficient calculations are presented in Fig. 3 (strong upper transition excitation) and Fig. 4 (weak excitation) as well. Symmetry prescribes that friction must be zero in a situation with both detunings equal to zero: there is no mechanism to generate a force in that situation. This no longer holds when a detuning δ_1 is applied in the excitation of the lower transition. The point where friction crosses zero is shifted in the case of strong saturation of the upper transition (Fig. 3). This has a dramatic effect since friction with a minus sign has the effect of exploding a sample of atoms in momentum space rather than confining them. For weak saturation of the upper transition, yet strong saturation of the lower (Fig. 4) it is seen that friction is negative for $\delta_1<0$ (curves b,c,d) for any value of δ_2. It is well known that in two-level molasses the friction coefficient changes sign in going to strong saturation. The high saturation of the lower transition explains the negative sign, and verifying the change of sign was used as a consistency check of the computer code.

Using the diffusion and friction results it is straightforward to calculate the temperature curves. As can be seen in Figs. 3 and 4 the scaled temperature does not go below 1, i.e., the Doppler limit for two-level excitation is never surpassed. We also made calculations for the case of weak infrared excitation and strong yellow excitation (not shown) and did not find any evidence for sub-Doppler temperatures.

These results can be used to explain some features in the experiments of Kumakura and Morita, as will be demonstrated in the next paragraph.

VII. COMPARISON WITH EXPERIMENTS

Kumakura and Morita performed precise fluorescence measurements for cascade excitation of metastable helium, varying laser detunings and powers [3]. The theory outlined above may be used to get a qualitative understanding of their observations.

The setup of the experiment is as follows. A magneto-optical trap (MOT) is loaded with metastable helium atoms from a Zeeman slower. The trapping laser beams are in a tetrahedral configuration and excite only the $2^3S_1\rightarrow 2^3P_2$ transition (1083 nm, infrared). Through the center of the trap, in one dimension, a pair of counterpropagating laser beams exciting the $2^3P_2\rightarrow 3^3D_3$ transition (588 nm, yellow) is applied. The trapping laser beams are circularly polarized, and the trap contains a mixture of m levels as a result of the MOT geometry, violating the ideal three-level situation. For qualitative analysis we will assume no coherences between different m levels, so that diffusion and friction will show the same qualitative behavior. We also assume that the Zeeman-

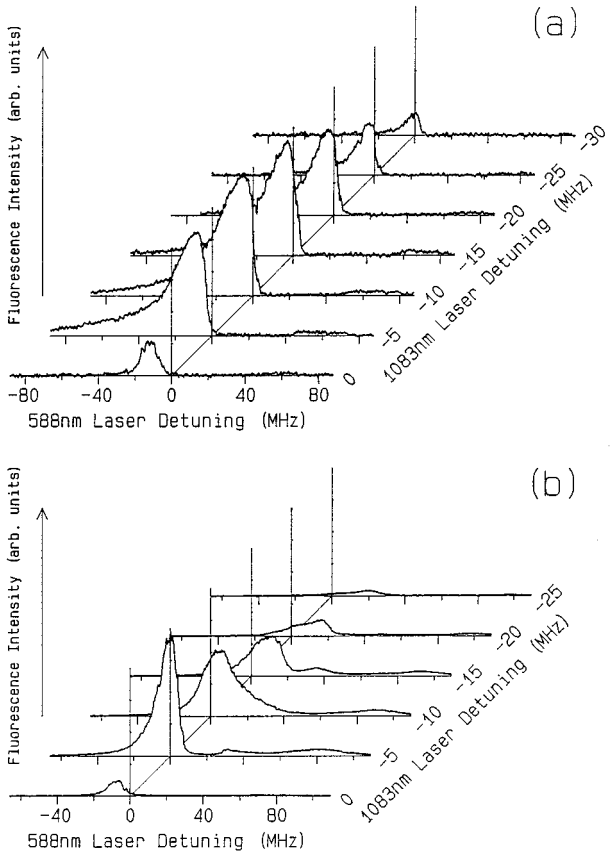

FIG. 5. Measurement of the 588 nm fluorescence of a cloud of metastable helium atoms trapped by 1083 nm laser beams ($\Omega_1=5.5\Gamma_1$), and intersected in one dimension by a standing wave of 588 nm radiation, as a function of the detuning of the two laser frequencies, both for strong excitation $\Omega_2=1.9\Gamma_2$ (a) and for weak excitation $\Omega_2=0.4\Gamma_2$ (b). Courtesy of Morita [3].

shift frequency introduced by the quadrupole field is small, and has no inhomogeneous effect on the fluorescence signal as a function of laser frequency. This is only the case for weak gradients and a relatively small sized cloud of atoms. The trap of Kumakura and Morita has a diameter of 1 mm.

The yellow laser introduces friction and diffusion in one dimension, which depend on detuning and intensity. These are the parameters that have been varied. The yellow fluorescence of the trapped atoms is shown in Fig. 5(a) (strong excitation for upper laser) and Fig. 5(b) (weak excitation). The Rabi frequencies are identical to those used to calculate Figs. 3 and 4.

At low intensity [Fig. 5(b)] the yellow laser is merely a perturbation and does not influence the dynamics of the MOT. The measured fluorescence is proportional to the population in the upper (3^3D_3) level, which indeed is small ($<5\%$). This population is maximal at two-photon resonance explaining the shift of the maximum in Fig. 5(b). Diffusion and friction effects due to the presence of the yellow laser cannot be tested in this situation. The observed maximum at $\delta_1=-5$ MHz is compatible with a reasonable population of the upper level at the best working conditions for the infrared MOT.

At high power the situation is notably different. Here $\Omega_2/\Omega_1=1.7$, which is close to the condition for maximum

force enhancement in overlapping traveling waves [11]. The effect of the yellow laser on the trap dynamics can be seen in the decrease of trap lifetime when Ω_2 is increased, as observed by Kumakura and Morita. Although the trap is three-dimensional and the yellow laser interacts only in one dimension, and is not overlapping with one of the infrared beams, most features in Fig. 5(a) may be explained using our one-dimensional theory. It is clearly seen in this figure that no trapping signal remains if the yellow laser is put on a positive detuning. This coincides with the situation in Fig. 3, where always ''anti''-friction ($\alpha<0$) occurs at positive yellow detuning. This leads to an explosion of the trap. It is interesting to consider the point where the friction crosses zero in Fig. 3. For the calculated values $|\delta_1|\neq 0$ this occurs for $\delta_2=-5$ MHz. This may explain the position of the maximum in Fig. 5(a). It is striking that a high maximum persists for increasing values of $|\delta_1|$, whereas the maxima decrease much faster in Fig. 5(b), as a function of $|\delta_1|$. The small signal in Fig. 5(a) for $\delta_1=0$ and $\delta_1<-20$ MHz can be explained by the fact that the loading of the MOT, that depends primarily on the four infrared laser beams, is ineffective: without the yellow laser hardly any atoms are trapped, as can be seen in Fig. 5(b) for $\delta_1=0$ and $\delta_1=-25$ MHz.

VIII. CONCLUSIONS

We presented a theory to calculate forces and diffusion and friction coefficients for a cascade level system. The results have been used to qualitatively explain our own experimental results as well as results of Kumakura and Morita. The cooling force, and thus the cooling rate, may be significantly larger than for traditional cooling on a two-level transition.

Neither in the numerical experiments, nor in the work of Kumakura and Morita do we find any evidence for sub-Doppler temperatures. The one-dimensional Doppler limit for the two-level system is derived for low saturation. However, high saturations for both the lower and the upper transition are required to obtain sufficient population of the upper state. In that case it appears that diffusion always increases more than friction, so that the equilibrium temperature increases too. This observation leads us to the conclusion that it seems not beneficial to use yellow laser beams to reduce the temperature in a trap (of course the issue of using it for increasing the loading rate or fluorescence probing is a different one).

It is possible to use the presented theory for multidimensional laser fields. In that case, however, it will be impossible to realize a pure three-level system, since more than one m component will be populated: the matrix A_p [Eq. (9)] will increase in size and will contain Clebsch-Gordan coefficients depending on the specific m values of the atom. We have carried out a laser cooling analysis for metastable helium moving in a traveling wave exciting the upper transition in one dimension and in a standing wave exciting the lower transition in the other dimension [26]. A system with 11 levels was obtained leading to a 121×121 matrix. As computing time for matrix inversion scales with n^3, the calculation of diffusion and friction coefficients becomes an extremely laborious job.

In the present paper diffusion and friction have been calculated for atoms with velocity close to zero. In general diffusion and friction display a rich and complicated behavior as a function of velocity, especially for high laser intensities, where Raman-like Doppleron processes play a significant role [27]. Calculating the full velocity dependence of these coefficients is hard but can nowadays be performed for one-dimensional standing waves, using continued fractions [28–30] or Floquet theory [31]. Similar work for a lambda three-level configuration has been performed by Drewsen [32]. However, the role of spontaneous emission is totally different from the case of cascade excitation. We are now incorporating these techniques in our computer code, and hope to describe our results in a future paper.

ACKNOWLEDGMENTS

We thank Nataly Konopleva and Anatoly Tumaikin from Novosibirsk State University for many fruitful discussions and Professor Morita for providing Fig. 5. Professor G. Nienhuis from the Universiteit Leiden is acknowledged for a critical reading of the manuscript. We gratefully acknowledge the financial support of the Foundation for Fundamental Research of Matter (FOM), which is part of the Netherlands Organization for Advancement of Research (NWO).

[1] J. Dalibard and C. Cohen-Tannoudji, J. Opt. Soc. Am. B **6**, 2023 (1989).
[2] A. Aspect, E. Arimondo, R. Kaiser, N. Vansteenkiste, and C. Cohen-Tannoudji, J. Opt. Soc. Am. B **6**, 2112 (1989).
[3] M. Kumakura and N. Morita, Jpn. J. Appl. Phys., Part 2 **31**, L276 (1992).
[4] R. Whitley and C. Stroud, Phys. Rev. A **14**, 1498 (1976).
[5] C. Cohen-Tannoudji, in *Fundamental Systems in Quantum Optics*, Les Houches Course XXX, 1990, edited by J. Dalibard, J. Raimond, and J. Zinn-Justin (Elsevier, Amsterdam, 1992).
[6] An ASCII file with all the expressions may be obtained by e-mail from one of the authors (W.R.).
[7] C. Cohen-Tannoudji and S. Reynaud, J. Phys. B **10**, 2311 (1977).
[8] R. Cook, Phys. Rev. Lett. **44**, 976 (1980).
[9] R. Cook, Phys. Rev. A **20**, 224 (1979).
[10] J. Gordon and A. Ashkin, Phys. Rev. A **21**, 1606 (1980).
[11] W. Rooijakkers, W. Hogervorst, and W. Vassen, Phys. Rev. Lett. **74**, 3348 (1995).
[12] T. Grove, B. Duncan, V. Sanchez-Villicana, and P. Gould, Phys. Rev. A **51**, R4325 (1995).
[13] J. Dalibard and C. Cohen-Tannoudji, J. Phys. B **18**, 1661 (1985).
[14] P. Ungar, D. Weiss, E. Riis, and S. Chu, J. Opt. Soc. Am. B **6**, 2058 (1989).
[15] G. Nienhuis, P. van der Straten, and S. Shang, Phys. Rev. A **44**, 462 (1991).
[16] K. Mølmer, Phys. Rev. A **44**, 5820 (1991).

[17] N. Konopleva and A. Tumaikin (Novosibirsk State University) have derived a Fokker-Planck equation for the specific case of a cascade system (unpublished).
[18] *Atomic, Molecular and Optical Physics Handbook*, edited by G. Drake (AIP, New York, 1996), pp. 879–880.
[19] A. Chu, D. Katz, M. Prentiss, M. Shahriar, and P. Hemmer, Phys. Rev. A **51**, 2289 (1995).
[20] G. Agarwal and K. Mølmer, Phys. Rev. A **47**, 5158 (1993).
[21] B. Renaud, R. Whitley, and C. Stroud, Jr., J. Phys. B **9**, L19 (1976).
[22] W. Ertmer, R. Blatt, J. Hall, and M. Zhu, Phys. Rev. Lett. **54**, 996 (1985).
[23] C. Salomon and J. Dalibard, C. R. Acad. Sci. **306**, Serie II, 1319 (1988).
[24] E. Korsunsky and Yu. Rozhdestvensky, Phys. Rev. A **52**, 3027 (1995).
[25] J. Guo and E. Arimondo, Phys. Rev. A **53**, R1224 (1995).
[26] W. Rooijakkers, W. Vassen, and W. Hogervorst (unpublished).
[27] N. P. Bigelow and M. G. Prentiss, Phys. Rev. Lett. **65**, 555 (1990).
[28] K. Berg-Sørensen, Y. Castin, E. Bonderup, and K. Mølmer, J. Phys. B **25**, 4195 (1992).
[29] T. Cai and N. Bigelow, Opt. Commun. **104**, 175 (1993).
[30] O. Emile, R. Kaiser, C. Gerz, H. Wallis, A. Aspect, and C. Cohen-Tannoudji, J. Phys. II **3**, 1709 (1993).
[31] R. Guccione-Gush and H. Gush, Phys. Rev. A **10**, 1474 (1974).
[32] M. Drewsen, Phys. Rev. A **51**, 1407 (1995).